

CHARACTERIZATION OF LARGE GRAIN Nb INGOT MICROSTRUCTURE USING OIM AND LAUE METHODS*

D. Kang, T.R. Bieler[#], D.C. Baars, MSU, East Lansing, MI 48823, U.S.A.

C. Compton, FRIB, East Lansing, MI 48823, U.S.A.

G. Ciovati, JLAB, Newport News, VA 23606, U.S.A.

T.L. Grimm, A. Kolka, Niowave Inc., Lansing, MI 48906, U.S.A.

Abstract

Large grain niobium (Nb) is being examined for fabricating superconducting radiofrequency (SRF) cavities as an alternative to using rolled sheet with fine grains. It is desirable to know the grain orientations of an Nb ingot slice before fabrication, as this allows heterogeneous strain and surface roughness effects arising from etching to be anticipated. Characterization of grain orientations has been done using orientation imaging microscopy (OIM, or electron backscattered pattern (EBSP) mapping), which requires destructive extraction of pieces from an ingot slice. Use of a Laue camera allows non-destructive characterization of grain orientations, a method useful for evaluating slices and deformation during the manufacturing process. Five ingot slices from CBMM, Ningxia, and Heraeus are examined. A pair of slices was deformed into two half cells and one of them was characterized again after deformation. The five ingot slices are compared in terms of their grain orientations and grain boundary misorientations. No obvious commonalities are indicated, which suggests that grain orientations develop randomly during solidification. A slab cut along the longitudinal direction of an Nb ingot was also examined, which showed the effect of machining on the grain orientations of the surface layer.

INTRODUCTION

Superconducting radio frequency (SRF) cavities fabricated from large grain Nb offers performance comparable to traditional fine-grain cavities [1-3]. The large grain approach allows simplification of the fabrication process, reduction of cost, and potentially better reproducibility in cavity performance [2]. Therefore, the SRF community has investigated this promising alternative fabrication path in recent years.

An important consideration arising from the large grain size is the mechanical and functional anisotropy associated with different grain orientations, which is discussed further in [3-5]. Therefore, characterization of

grain orientations in an ingot slice is necessary prior to fabrication in order to anticipate potential forming problems and relationships between forming history and eventual performance.

EXPERIMENTS

OIM and Laue Methods

Being a well-established technique to measure grain orientations, OIM has been used to characterize ingot slices. However, this requires extracting small pieces from a slice, and thus makes the slice essentially unusable for cavity fabrication. The Laue Method based on X-ray diffraction provides a non-destructive alternative method to measure grain orientations.

Laue measurements do not need to be performed in vacuum, which greatly loosens the geometrical restrictions imposed by the chamber of an electron microscope. Therefore, samples with larger or more complicated dimensions can be characterized. Also, unlike in OIM where only “representative” locations are measured, the Laue method enables measurements from virtually anywhere on an ingot slice, and the ingot slice can be evaluated at various stages along the fabrication path. A more detailed discussion on both methods and their intrinsic accuracy is presented in [3, 6-7].

Measurements of Grain Orientations

Two ingots slices from CBMM and Ningxia were characterized with OIM (Fig. 1). An ingot slice produced by Heraeus (Fig. 1), and another two ingot slices from CBMM (denoted H1 and H2 respectively) were examined by the Laue method. H1 and H2 were cut right adjacent to each other, and the difference between them is very small as indicated by the results in Table 1. Consequently only H1 is shown in Fig. 1. Mounting error should only affect measurements in the first Euler angle, so the orientation variations presented are representative of real orientation gradients.

H1 and H2 were deep drawn into half cells and H2 was characterized again by the Laue method after deformation (Fig. 2).

A longitudinal Nb slab prepared by Niowave (Fig. 3) was also characterized with the Laue method. After a coarse saw cut, the slab was given a smooth surface using an end mill, and then mechanically polished to make the grains on the surface clearly visible.

* This work was funded by a research contract DE-S0004222 from DOE-OHEP. The Heraeus ingot slice was provided by DESY (W. Singer), the CBMM ingot slice was provided by Jefferson Lab (P. Kneisel), the Ningxia ingot slice was provided by the National Superconducting Cyclotron Laboratory (C. Compton), ingot slices H1 and H2 were provided by Jefferson Lab (G. Ciovati), and the ingot slab was provided by Niowave Inc. (T.L. Grimm)

[#]bieler@egr.msu.edu

Orientation maps were constructed with the aid of EDAX/TSL analysis software, by assigning measured orientations to pixel positions obtained from optical images of the ingot slice [3].

RESULTS

Measured grain orientations are overlaid onto the images of several ingot slices in Fig. 1. Table 1 lists the orientations for H1 and H2 before deep drawing, which indicates that orientation gradient is small not only within the large grains for each slice, but also between H1 and H2. The orientation maps are shown in Fig. 4, with prisms showing corresponding grain orientations. Density pole

figures and normal direction discrete inverse pole figures (IPFs) are shown in Fig. 5. A misorientation distribution function (MODF) is also generated for each ingot slice (Fig. 6), where each section represents the distribution of rotation axes for each of the binned grain boundary misorientation angle ranges indicated. For comparison, the actual misorientation axes between grains are marked using X's in Fig. 6, and are annotated on the images of the slices in Fig. 1.

Fig. 2 shows the orientations of the deformed half cell H2 (in yellow), at locations numbered from 1 to 12. Here, a different numbering is used because the locations chosen do not always match those on the undeformed

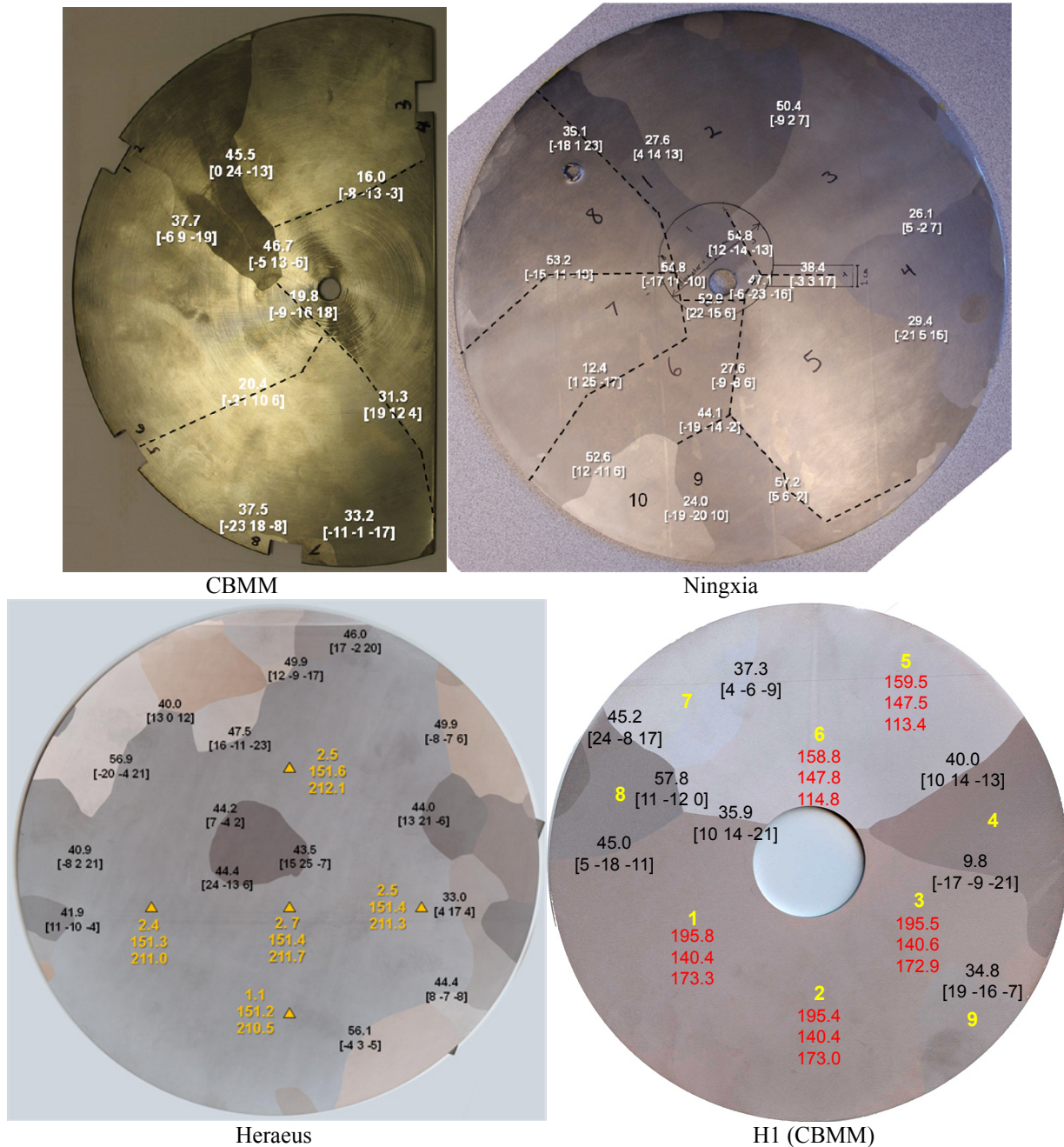


Figure 1: Images of the ingot slices examined. Annotation provides angle [axis] grain boundary misorientation, and Euler angles.

slice. Each orientation was measured with its local surface normal parallel to the incident X-ray beam. As a comparison, orientations prior to deformation are presented in black.

Fig. 3(a) shows the characterized ingot slab. Grain orientations were measured at the numbered locations. 10 closely spaced orientations were made to the left of orientation 2 across two milling passes (Fig. 3(b)), where orientation *j* was about halfway between orientations 2 and 27. A normal direction OIM map was constructed in Fig. 3(c); note that the surface normal of the slab would be perpendicular to the surface normal of an ingot slice.

Table 1: Grain orientations of H1 and H2 (CBMM).

	H1			H2		
1	195.8	140.4	173.3	195.3	140	173.4
2	195.4	140.4	173	195.7	140.3	172.9
3	195.5	140.6	172.9	195.5	139.8	172.9
4	29.2	134.7	181.6	29.3	135.2	182.2
5	159.5	147.5	113.4	160.3	147.4	113.7
6	158.8	147.8	114.8	159.4	147.6	114.2
7	206.5	158.8	126.5	205.2	158.5	125.4
8	248.5	128.9	187.9	248.1	128.9	188.3
9	135.7	154.7	130.6	136.4	153.8	132

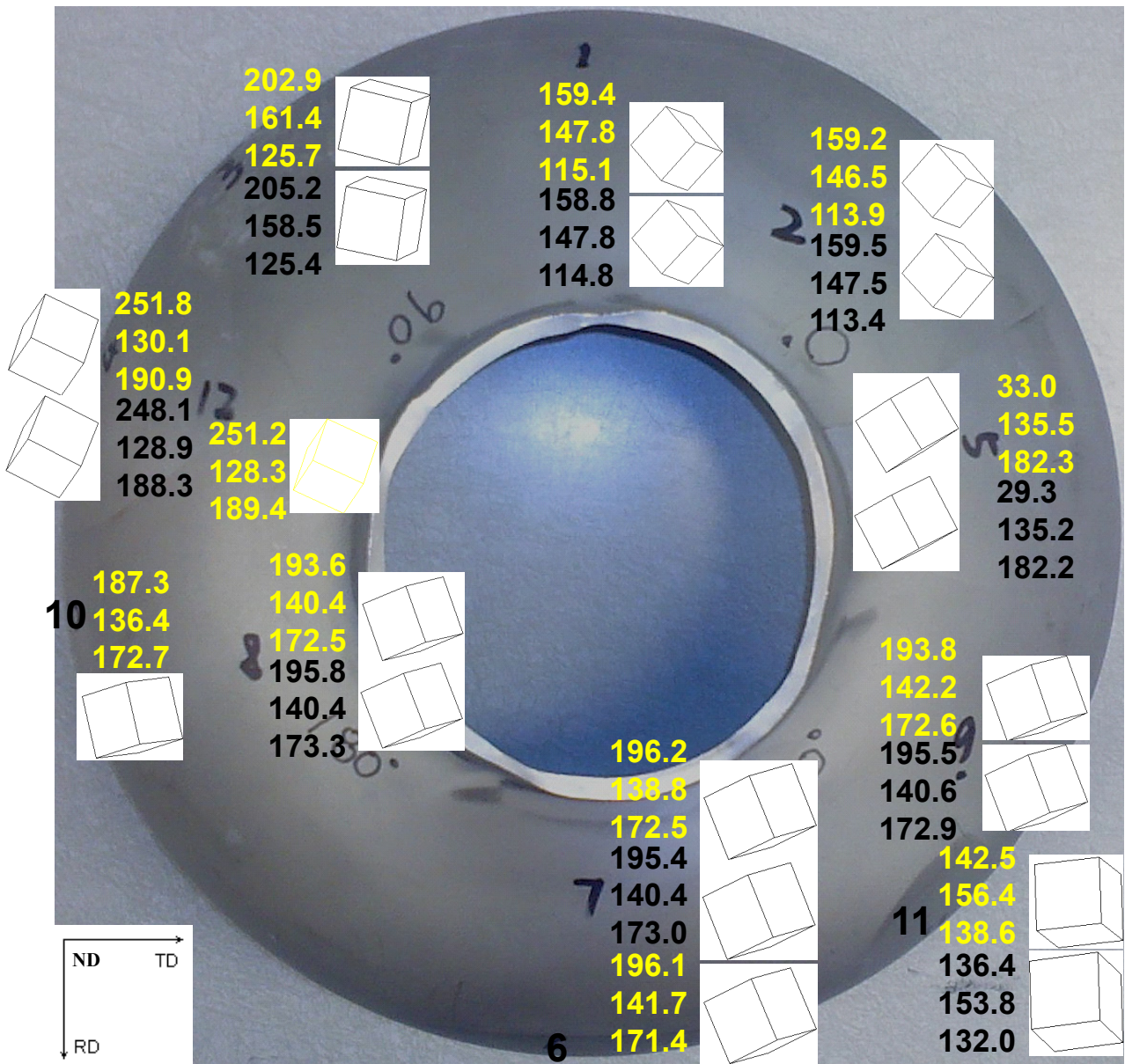


Figure 2: A half cell that is deep drawn from ingot slice H2 (CBMM). Grain orientations measured before and after deformation are overlaid onto the image (yellow – after, black – before).

DISCUSSION

Similarities and Differences Among Ingot Slices

The five ingot slices are compared in terms of their grain orientations and orientations distributions. The pole figures and inverse pole figures in Fig. 5 show no obvious

similarities, suggesting that there is no preferred orientation that is intrinsic to processing Nb ingots. From the orientation map, it is possible to develop misorientation distribution plots in Fig. 6. There is a preference for grain misorientations between 35-55° (marked by X's in Fig. 6). For a completely random

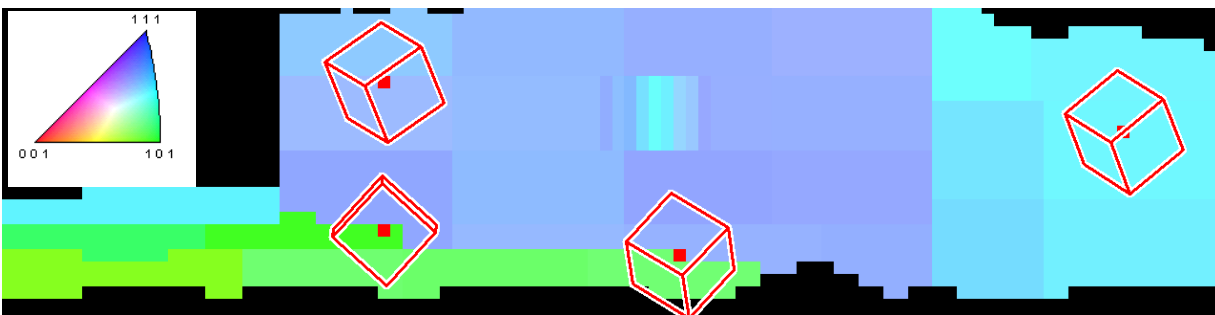


Figure 3: (a) Image of the longitudinal ingot slab (about 110cmx30cm in dimension). (b) Finer scans to the left of location 2 across one milling band. (c) Normal direction orientation mapping using a 100x26 grid on the slab.

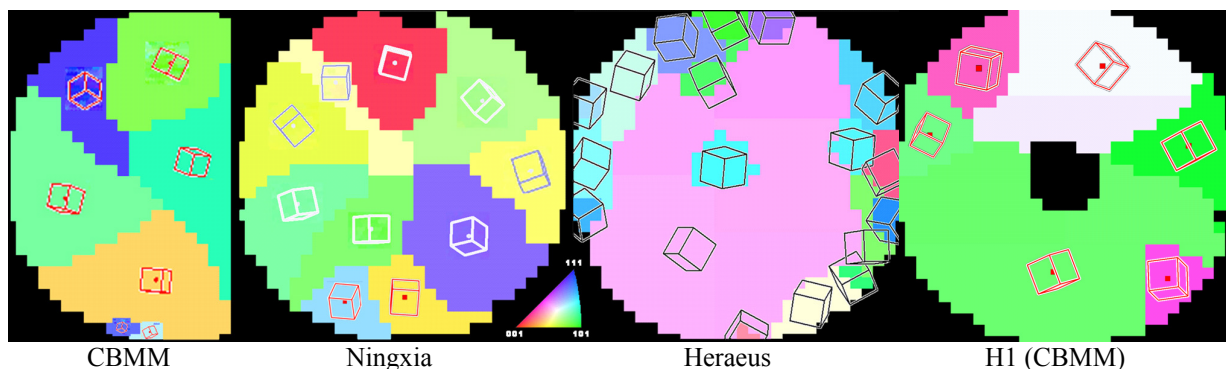


Figure 4: Normal direction orientation mapping using a 30x30 grid on the ingot slices.

distribution of orientations in cubic polycrystals there is high probability of misorientations between 35-55° with a maximum at 45° [8]. Also there is no commonality in orientation, grain boundary misorientation, or grain size among the ingots examined here and a characterization of a different Heraeus ingot slice [9]. These observations suggest that there is no highly preferential grain boundary mobility or interfacial energy that would cause a bias in grain orientations or grain boundary misorientations.

Fig. 7 shows maximum Schmid factor maps based upon biaxial deformation (which is a convenient estimate for strains likely in a formed half cell) for each ingot slice, for slip on {110}, {112}, or both families of planes, as both are equally facile [10]. The (dark) orientations have the lowest Schmid factor arising from the [111] direction normal to the surface. This orientation requires greater stress to deform, and while it strains more uniformly than the softer orientations [10], this benefit would only be

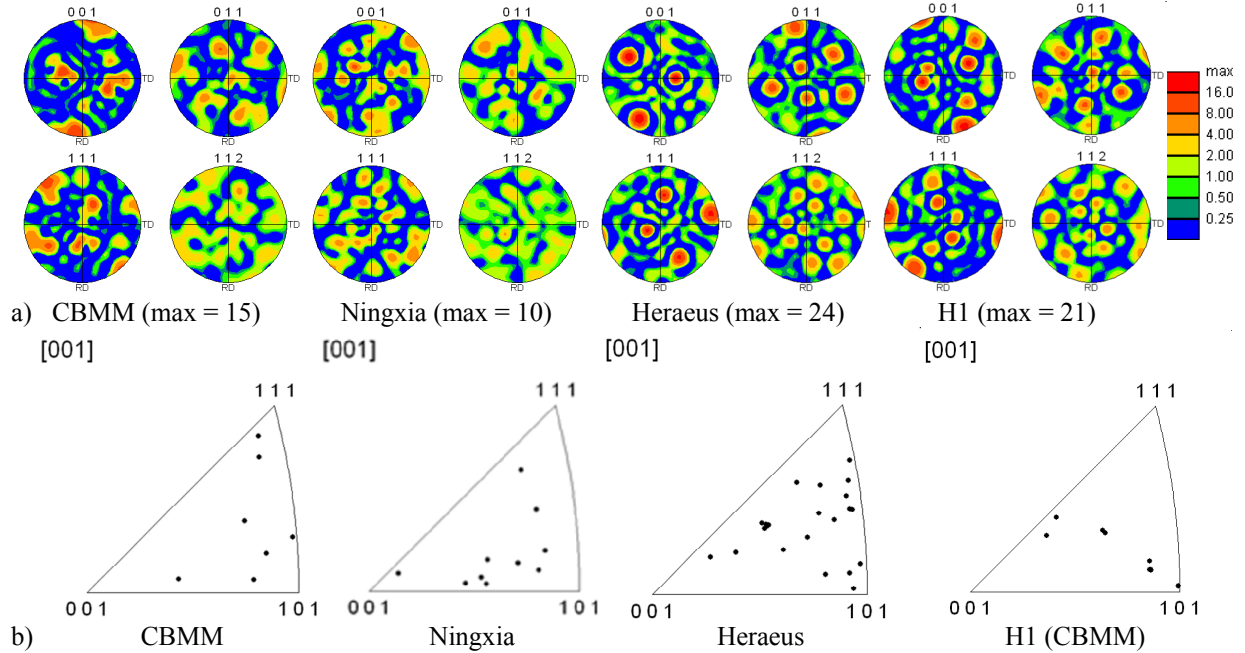


Figure 5: a) Density pole figures and b) Surface normal direction discrete inverse pole figures for each ingot slice.

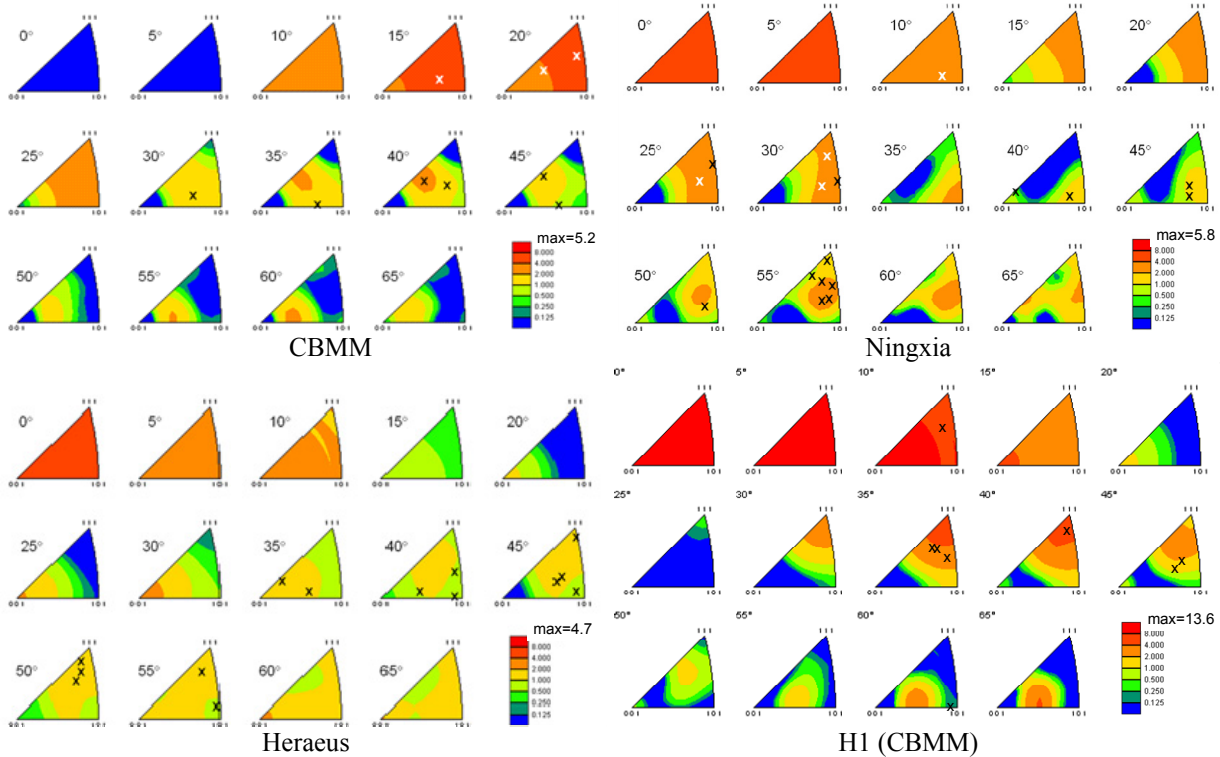


Figure 6: Grain boundary misorientation distribution function (MODF) for the four ingot slices.

gained if there were no soft orientations. Hence, a mixture of soft and hard orientation would lead to very non-uniform deformation in the grain boundary regions. Thus the Heraeus and the H1 (and H2) slices would be expected to provide the most homogeneous deformation, as there is no grain that is intrinsically hard (dark); this is confirmed by the deformed half cell in Fig. 2 which shows very little evidence for non-uniform strain.

Another issue is the orientation gradient within the large grains. In the Heraeus and H1 (H2) slices, very little variation in orientations is detected, while much larger variation is found in the CBMM and Ningxia slice [3]. It is not yet clear as to how this orientation gradient came about and how it would eventually affect cavity performance.

Effect of Deep Drawing on Grain Orientations

A typical cavity fabrication process involves deep drawing of ingot slices into cup-shaped half cells (Fig. 2), and the half cells are then electron beam welded together to form a cavity. Ideally, the mechanical properties should be isotropic in the plane of the slice, which is not necessarily the case for large grain ingot slices [11]. It is therefore important to examine how preexisting anisotropy affects deformation. A preliminary assessment is made by comparing grain orientations before and after deformation.

No significant changes in orientations were observed at all of the locations shown in Fig. 2. This agrees with the formability prediction from Fig. 7 that all grains are relatively soft and would deform similarly. No obvious grain boundary ledges or severe surface topography were present either, which again suggests that all grains deformed similarly. The center grains would be of greater

importance in terms of formability as the iris region experiences the most strain during deep drawing. The irregularities at the center and on the perimeter are the consequence of anisotropic flow, causing “earring”, which requires trimming after the deep drawing process.

Grain orientations along the radial direction were also investigated, in that the stress state varies from iris to equator region. Three such pairs were chosen (12→4, 8→10 and 7→6 in Fig. 2). Changes in orientations were constantly observed as expected, with varying magnitude. Future work will use strain tensors obtained from finite element modeling of the deep drawing process to assess which slip systems were activated. This analysis will provide the means to compare simulated and measured changes in crystal orientation, to assist in constitutive model development.

The azimuthal asymmetry in the formed half cells associated with anisotropy is non-negligible, as any shape irregularity requires special jigs or secondary forming operations prior to welding. Since the grain orientations do not change much from one ingot slice to an adjacent one (Table 1), it might be practical to use a series of adjacent ingot slices to form a serial set of half cells that belong to one cavity, and align them so as to match grain boundary positions. However, welding of deformed large grains causes recrystallization as illustrated in [12], but the influence of welds in matched grain orientations has not been examined.

A comparison of Laue diffraction patterns before and after deep drawing (Fig. 8) shows a clear effect of deformation. The distinct diffraction spots became smeared after deformation, indicating that a large amount of crystal defects (mainly dislocations) have been generated, which are known to increase residual surface

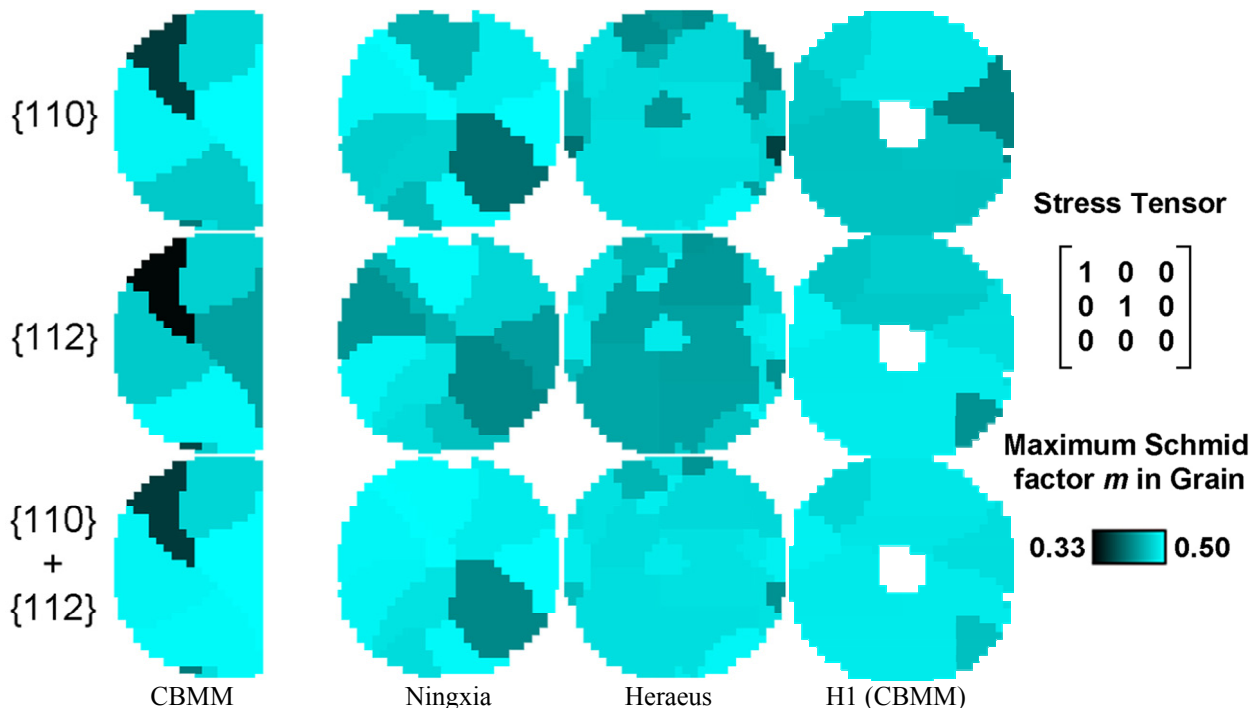


Figure 7: Schmid Factor maps for slip on {110}, {112} or both families of planes based upon biaxial tension.

resistance and degrade cavity performance [13]. Heat treatments are effective in reducing defect density and improve RRR and thermal conductivity values [14].

Effect of Heavy Machining on Grain Orientations

A common practice for post processing of fine-grain cavities is to remove a surface layer of at least $100\mu\text{m}$ to get rid of a damaged layer [11]. The measurements on the Nb ingot slab provide additional information about the effect of surface damage on crystal perfection. The orientation of the large grain only varied slightly from one end to the other along the longitudinal direction, but enough to cause a noticeable change in color on the map. There is a periodic oscillation that comes from the milling band. For example, if orientation 11 (left side) is used as reference, the misorientations for orientations 4, 2 and 1 (along a milling band near the center) are 6.4° , 6.5° and 6.8° , respectively. The orientations 9, 24 and 22 (right end) along a different milling band have much smaller misorientations of 1.6° , 1.2° and 1.2° , respectively. The six orientations measured on the right end are measured on the same milling direction pass, but it is the opposite direction from all of the measurements on middle and left end of the slab. The orientations are correspondingly similar in bands milled in the same direction. Thus, a

finer step set of orientations to the left of orientation 2 were measured to identify this periodicity. Using orientation 2 as a reference, the misorientation reaches a peak (6.8°) around the center of the adjacent band (f), and then gradually drops to a small value at position j (0.7°). Orientation j is close to orientation 27, which had the same milling direction. This oscillation is represented in the orientation map, which shows a color change that is correlated with milling pass direction.

This periodicity of misorientations arising from machining effects provides one possible explanation for the necessity of chemical surface removal after cavity fabrication. To examine this issue further, one end of the slab will be etched to remove about $100\mu\text{m}$, and the surface orientations and crystal perfection will be assessed to determine if the oscillation in orientation and hence, the surface damage layer was removed.

If the orientation of the large grain truly does not vary much from one end to the other, then it would be possible to extract a large number of ingot slices with similar crystal orientations. Nevertheless, whether this apparent consistency in grain orientations is typical among Nb ingots remains an open question.

Another observation regarding surface damage is that smearing of diffraction spots is not evident in most of the

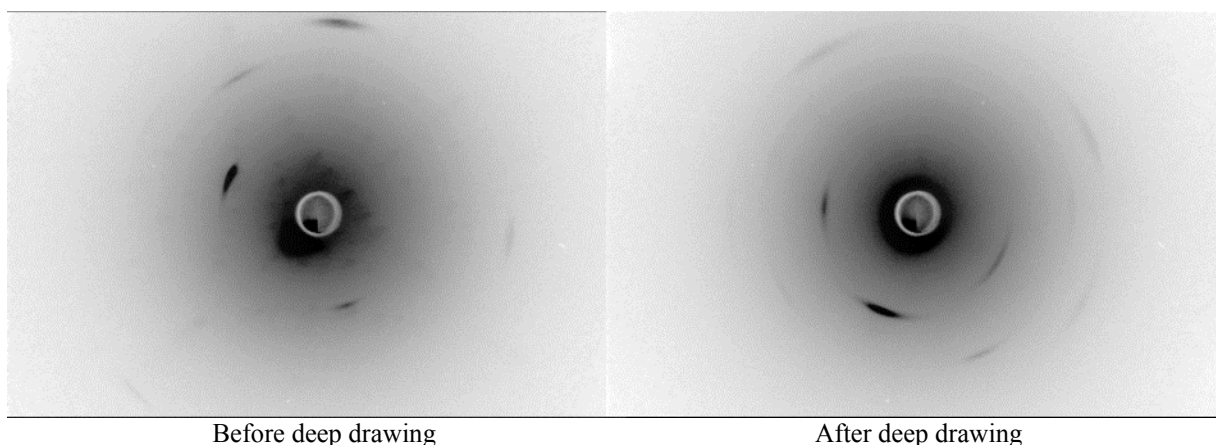


Figure 8: Laue diffraction patterns from roughly the same location before and after deep drawing on H2, showing how distinct diffraction spots disappeared after deep drawing.

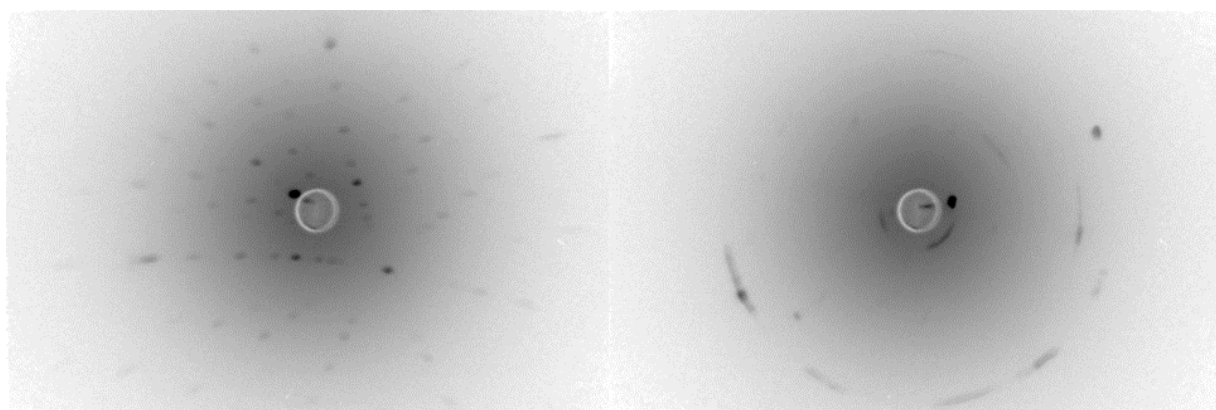


Figure 9: Two Laue diffraction patterns from the ingot slab. The left pattern shows distinct diffraction spots from the middle of a milling band, and the right pattern shows smearing of spots from the edges of milling bands.

diffraction patterns in the ingot slab (Fig. 9; smearing is only found at the edges of the milling bands). This uniform peak shift instead of peak broadening suggests that end milling produces a more uniform macro strain (note that polishing probably removed some degree of surface damage arising from friction effects with the tool). On the other hand, the deep drawn half-cell was not polished, and localized surface friction interactions with the die may have caused varying micro-strains that led to peak broadening [7].

CONCLUSIONS

Five Nb ingot slices were characterized using the OIM or Laue method. The results indicate that there are no obvious commonalities among ingots from different suppliers, or among different ingots from the same suppliers. Furthermore, there is no obvious preference for particular orientations or grain boundary misorientations, suggesting that the solidification process is dominated by random mechanisms. From the observations of the longitudinal ingot slab, grain orientations appear to be consistent along the longitudinal direction.

Effects of plastic deformation on grain orientations were examined. Heavy machining such as end milling is likely to introduce uniform strain, while friction effects from deep drawing may produce more localized strain. Both can lead to surface damage and a subsequent chemical surface removal is necessary.

Use of a Laue camera to nondestructively measure grain orientations is a promising alternative to OIM. Ingot slices can be evaluated at various stages along the fabrication path, and can provide some metallurgical perspectives that can be correlated with cavity performance. The Laue method could also be used to characterize grain orientations in the heat affected zone of equator welds on SRF cavities [15].

REFERENCES

- [1] G. Ciovati, P. Kneisel, G.R. Myneni and S. Chattopadhyay, Performances of high-purity niobium cavities with different grain sizes, Proceedings of LINAC 2006 (JACoW), TUP033, pp. 318-20.
- [2] P. Kneisel, Review of progress on large grain and single grain niobium cavities, Proceedings of SRF2007, Peking Univ., Beijing, China, paper TH102.
- [3] D. Kang, D. Baars, T. Bieler and C. Compton, Characterization of large grain Nb ingot microstructure using EBSD mapping and Laue camera methods, AIP Conf. Proc., 2011, Volume 1352, pp. 90-99.
- [4] D. Hull and D.J. Bacon, Introduction to Dislocations (Butterworth-Heinemann, Oxford, 2001), 4th Ed.
- [5] D. Baars, T. Bieler, P. Darbandi, F. Pourboghra, C. Compton, SRF09, 14th International Conference On RF Superconductivity, SRF2009 WEB Proceedings, ISSN 1868—5781, pp.144-48.
- [6] EDAX/AMETEK, Inc., Introduction to Orientation Imaging Microscopy.
- [7] B.D. Cullity and S.R. Stock, Elements of X-ray diffraction, Third edition, Prentice Hall 2001, Upper Saddle River, NJ.
- [8] J.K. Mackenzie, *Biometrika* 45 (1958), p. 229.
- [9] W. Singer, A. Brinkmann, A. Ermakov, J. Iversen, G. Kreps, A. Matheisen, D. Proch, D. Reschke, X. Singer, M. Spiwek, H. Wen, H.-G. Brokmeier, Single Crystal—Large Grain Niobium Technology, International Niobium Workshop, 2007 American Institute of Physics Proceedings 927, pp. 123-32.
- [10] T.R. Bieler, N.T. Wright, F. Pourboghra, C. Compton, K.T. Hartwig, D. Baars, A. Zamiri, S. Chandrasekaran, P. Darbandi, H. Jiang, E. Skoug, S. Balachandran, G. E. Ice, and W. Liu, *Physical Review Special Topics - Accelerators and Beams* 13, 031002 (2010).
- [11] D. Proch, RF Cavities Fabrication, DESY, Hamburg, Germany.
- [12] T.R. Bieler, N.T. Wright, F. Pourboghra, C. Compton, K.T. Hartwig, D. Baars, A. Zamiri, S. Chandrasekaran, P. Darbandi, H. Jiang, E. Skoug, S. Balachandran, G.E. Ice, and W. Liu, *Physical Review Special Topics - Accelerators and Beams* 13, 031002 (2010).
- [13] CERN Accelerator Schools: Superconductivity in Particle Accelerators “Yellow reports” n. 89-04 and 96-03.
- [14] S. Chandrasakaran, N.T. Wright, T.R. Bieler, C. Compton, this proceedings.
- [15] D. Baars, H. Jiang, T.R. Bieler, C. Compton, T.L. Grimm, *IEEE Transactions on Applied Superconductivity* 17 1295-1298 (2007).